American Mineralogist, Volume 93, pages 1574–1580, 2008

New data on PGE alloy minerals from a very old collection (probably 1890s), California

Andrei Y. Barkov,[1] Robert F. Martin,[1,*] Lang Shi,[1] and Mark N. Feinglos[2]

[1]Department of Earth and Planetary Sciences, McGill University, 3450 University Street, Montreal, Quebec, H3A 2A7, Canada
[2]Box 3921, Duke University Medical Center, Durham, North Carolina 27710, U.S.A.

Abstract

We report results of multiple electron-microprobe analyses of nine grains of alloy minerals, 2–5 mm in size, rich in the platinum-group elements (PGE), from a unique, very old collection (~1890s) of placer material from Trinity Co., California. Osmium, iridium, ruthenium, and rutheniridosmine are the principal alloy species poor in Fe (typically <0.5–1 wt%); they appear to be primary. An Fe-enrichment (up to 4.6 wt%) is observed in lamellae of Ir-Ru-Os alloy exsolved from the Fe-poor Os-Ir-Ru alloy host, and also in a rim-like alteration-induced phase developed along the margin in some of the grains of Ir-Ru-Os alloy. Much greater levels of Fe (up to 19.1 wt%), incorporated via the substitution mechanisms: Fe → Ru, Fe → (Os + Ru), and Fe → Ir, were documented in three grains of Fe-Os-Ru-Ir alloys, which attain Fe-dominant compositions, i.e., hexaferrum. These Fe-Os-Ru-Ir alloys and associated exotic phases enriched in unconventional elements, such as W-(Mo)-bearing rutheniridosmine, $(Os,Ir)_5(W,Mo)$ and newly recognized $(Ir,Os)_5(W,Mo)$, appear to be secondary, formed under conditions of low fugacities of O_2 and S_2 as a result of interaction of primary Os-Ir-Ru alloys with a reducing fluid phase. No grains of Pt-Fe alloys were found; these only occur as Pt_3Fe-type (isoferroplatinum or Fe-rich platinum) and Pt_2Fe-type inclusions (<50 μm), enclosed in a matrix of Ir- or Os-dominant alloys rich in Ru. The Pt_2Fe alloy appears to be a compositional variant of Fe-rich platinum, possibly reflecting a lower limit of Pt content possible in the mineral platinum. An Au-Ag alloy, ranging up to $Au_{0.99}$, precipitated pseudomorphously by a subsolidus reaction between a residual Au-Ag-rich melt and exsolution-induced inclusions of the Pt-Fe alloy phases. Micro-inclusions of olivine, hosted by a ternary alloy $Os_{0.33}Ru_{0.33}Ir_{0.30}$, are extremely rich in Mg ($Fo_{95.1–95.4}$), probably reflecting high-temperature reaction involving chromite or magnesiochromite. The alloy grains from the old collection were likely derived from a mineralized zone of ultramafic rocks, rich in chromite-magnesiochromite and poor in overall S, in the Trinity ophiolite complex of northern California.

Keywords: PGE alloy minerals, old collection, Trinity ophiolite complex, northern California

Introduction

Recently, a unique alloy mineral of Os, Ir, W, and Mo corresponding to a formula $(Os,Ir)_5(W,Mo)$, was reported from California in association with an unusual Os-Ru alloy enriched in Fe (up to 9.7 wt%; Barkov et al. 2006). This association between the platinum-group elements (PGE) and W-Mo, which differ in their geochemical and crystallochemical properties, is extraordinary, as also is a strong enrichment in Fe in a group of naturally occurring Os-Ru-Ir-based alloys. These unusual grains of PGE-rich alloys form part of a very old collection of placer minerals, owned by one of the authors (M.N.F.) and preserved in the original vial. This collection was gathered approximately in the 1890s; a more recent label provided with these samples records the locality as "Trinity Co., California."

In the present paper, we report results of a further study, based on a total of 550 electron-microprobe analyses obtained for nine grains of PGE alloy minerals from the old collection. We follow principles of the IMA-accepted nomenclature for PGE alloy minerals (Cabri and Feather 1975; Harris and Cabri 1991; Cabri 2002), avoiding prefixes such as "ferroan," etc., as was recently recommended by the IMA (Bayliss et al. 2005). Our study resulted in the identification of various alloy minerals, described here, along with the analyzed micro-inclusions of olivine ($Fo_{95.1–95.4}$), Pt_2Fe- and Pt_3Fe-type alloys, and of Au-Ag alloy, all hosted by Os-Ir-Ru alloys. Several of the newly identified alloys are especially interesting. Hexaferrum (Fe,Os,Ru,Ir) is a complex and exceptionally rare Fe-dominant solid-solution (up to 19.1 wt% Fe), previously unreported from North America. We encountered a new compound, $(Ir,Os)_5(W,Mo)$, that appears to be an Ir-dominant counterpart of the unnamed $(Os,Ir)_5(W,Mo)$. We describe the extent of compositional variations observed for grains of various Fe-Os-Ir-Ru alloy minerals from the old collection. On the basis of new results, we discuss some aspects of the crystallization history of these alloy minerals, placer grains of which were probably derived from the Trinity ophiolite complex of northern California.

The Trinity complex of peridotite and associated gabbro is Ordovician in age; it forms the structural base of the eastern Klamath plate in the Klamath province, northern California and southern Oregon (Peacock 1987, and references therein).

Electron-microprobe analyses

Electron-microprobe (EMP) analyses of alloys of the PGE and Au-Ag were carried out using a JEOL JXA-8900 instrument (McGill University) in wavelength-dispersive spectrometry mode (WDS) at 20 kV and 30 nA, with a finely focused

* E-mail: bobm@eps.mcgill.ca

beam (1–2 μm) and ZAF on-line correction procedures. Pure Os, Ir, Ru, Rh, Pt, Pd, Fe, Ni, Co, W, Mo, $CuFeS_2$ (for Cu), and $Au_{60}Ag_{40}$ were used as standards. In analyses of PGE-rich alloys, the $L\alpha$ line was applied for Ir, Pt, Rh, Ru, W, and Mo, the $M\alpha$ line for Os, the $L\beta$ line for Pd, and the $K\alpha$ line for Fe, Ni, Co, and Cu. In analyses of Au-Ag alloy, the $M\alpha$ line was applied for Au and the $L\alpha$ line for Ag and Cu. Inclusions of olivine were analyzed at 20 kV and 20 nA (WDS), using a set of well-characterized standards. All possible peak-overlaps among the X-ray emission lines employed were checked and corrected.

RESULTS

Compositions of Os-Ir-Ru, Fe-Os-Ir-Ru, and W-(Mo)-Os-Ir-Ru alloys

The samples analyzed in this study are typically roundish alloy grains, in some cases with relics of faceted morphology (Fig. 1a); they range up to 5 mm across. Grains of Fe-rich Os-Ir-Ru alloy are porous (Figs. 1b and 1c), as is also reflected in their lower totals of EMP analyses.

Our compositional data, obtained for grains of Os-Ir-Ru alloys, are clustered in different areas of the Os-Ru-Ir system (Fig. 2), indicative of four mineral species. In accordance with the nomenclature of Harris and Cabri (1991): (1) osmium is hexagonal with Os as the major element; (2) iridium is cubic with an Ir-dominant composition; (3) ruthenium is hexagonal, where Ru is the major element; and (4) ruthenirid osmine is hexagonal with Ir > Os or Ru. Thus, these four species are the principal phases in most of the analyzed grains. The abundance of Ru-enriched alloys is especially noteworthy (Fig. 2; Tables 1 and 2); this feature is consistent with the reported occurrence of a nugget of Os-Ir alloy rich in Ru in stream gravels of the Trinity River (Snetsinger 1971).

These grains of alloys of Os, Ru, and Ir, which appear to represent primary phases, are poor in Fe (typically <0.5–1 wt% and up to 1.5 wt%). In contrast, a relative enrichment in Fe is observed in two textural varieties of alloy, both of which presumably formed relatively late in the crystallization history: (1) narrow lamellae of Ir-Ru-Os alloy exsolved from the Fe-poor Os-Ir-Ru alloy host, and (2) an alteration-induced phase, which is rim-like (up to 20 μm thick), developed along the margin in some of the Ir-Ru-Os alloy grains. Because of the presence of elevated Fe (3.7–4.6 wt%), such lamellae are gray in back-scattered electron images, BSE (Fig. 1d). Compositions of several lamellae are in the range $Ir_{0.38–0.41}Ru_{0.31–0.32}Os_{0.12}Fe_{0.10–0.12}Pt_{<0.01–0.04}Rh_{0.02–0.03}$ (basis: Σ atoms = 1). The host alloy, $Os_{0.33}Ru_{0.33}Ir_{0.30}Pt_{0.03}Rh_{0.01}Fe_{<0.01}$, has about the same content of Ru, is nearly devoid of Fe, and richer in Os but poorer in Ir. It appears from these data that (Fe + Ir) replaces Os in the lamellar phase. The alteration-induced phase (also gray in BSE imaging) and the original alloy before alteration have the compositions $Ir_{0.43}Ru_{0.31}Os_{0.18}Fe_{0.07}Rh_{0.01}$ and $Ir_{0.44}Ru_{0.36}Os_{0.17}Fe_{0.02}Rh_{0.01}$, respectively. Here, a Fe-for-Ru mechanism of substitution is implied. Both Fe-bearing Ir-Ru-Os phases gave lower totals (anal. 12, Table 1), which are ascribed to their porous texture. In addition, our EMP data suggest that up to 7.5 wt% Au may be present in the composition of some of Fe-bearing Ir-Ru-Os alloy phases.

Much greater levels of Fe (up to 0.41 apfu, Table 2) are observed in three grains of composite Fe-Os-Ru-Ir alloys, which range up to Fe-dominant compositions, corresponding to the mineral hexaferrum. Our results of EMP analyses, obtained for three separate alloy grains of the hexaferrum-rich solid solution, yield three series of compositions (Figs. 3a–3d). One of these grains is in fact a rim developed around a core of Os-rich iridium: $Ir_{0.56}Os_{0.20}Ru_{0.11}Pt_{0.06}Rh_{0.05}Fe_{0.01}$ (Fig. 1c). The composition of this rim phase is rich in Ir (up to 0.40 apfu Ir: Fig. 3c), reflecting the Ir-rich composition of the primary alloy (i.e., the core). The other two analyzed grains of hexaferrum are rich in Ru, and differ in their amounts of Fe. Their compositional trends are subparallel, having a similar slope and length. Also, they have

TABLE 1. Compositions of Os-Ir-Ru alloys from the old collection, California

	Cu	Co	Fe	Ni	Pt	Ir	Os	Pd	Rh	Ru	Total
1	0.01	0.01	0.13	0.02	5.85	16.24	51.42	0.24	2.00	23.11	99.04
2	0	0.01	0	0	0.06	8.51	84.58	0.15	0.11	6.86	100.27
3	0	0	1.25	0.14	4.69	86.56	5.94	0.07	0.39	2.14	101.17
4	0	0	0.22	0.01	0.98	33.91	54.20	0.07	0.50	10.81	100.69
5	0.05	0.01	0.07	0.01	4.07	34.46	38.89	0	0.85	21.12	99.53
6	0	0.02	0.06	0.02	5.01	30.94	38.81	0	0.88	23.73	99.46
7	0.11	0.10	0.02	0	0.67	47.97	25.27	0.03	1.13	23.77	99.07
8	0.14	0	1.46	0	8.10	57.78	11.76	0.04	2.25	17.62	99.14
9	0.02	0.01	0.68	0.11	0.04	54.32	20.17	0.02	0.83	23.59	99.79
10	0	0	0.81	0.17	1.86	47.43	23.94	0	0.90	24.72	99.83
11	0.06	0.01	0.39	0.10	7.14	60.64	21.49	0	3.13	6.35	99.30
12	0.04	0.02	4.04	0.06	4.50	49.64	15.64	0	1.91	21.50	97.36
at%											
1	0.03	0.04	0.35	0.06	4.70	13.24	42.35	0.36	3.04	35.82	100
2	0	0.03	0	0	0.05	7.91	79.45	0.25	0.19	12.13	100
3	0	0	4.03	0.43	4.32	81.01	5.62	0.11	0.67	3.81	100
4	0	0	0.69	0.02	0.86	30.26	48.89	0.11	0.83	18.35	100
5	0.12	0.03	0.19	0.04	3.34	28.72	32.76	0	1.32	33.48	100
6	0	0.05	0.16	0.04	4.04	25.32	32.10	0	1.34	36.94	100
7	0.26	0.27	0.05	0	0.54	39.24	20.89	0.05	1.73	36.98	100
8	0.35	0	4.16	0	6.60	47.80	9.83	0.05	3.48	27.72	100
9	0.06	0.02	1.88	0.30	0.03	43.81	16.44	0.03	1.25	36.18	100
10	0	0	2.21	0.45	1.46	37.80	19.28	0	1.34	37.46	100
11	0.16	0.02	1.23	0.28	6.44	55.54	19.89	0	5.35	11.06	100
12	0.10	0.06	10.81	0.15	3.45	38.59	12.29	0	2.77	31.79	100

Notes: The selected results of WDS electron-microprobe analyses (JEOL JXA-8900 microprobe) are listed in wt% and in at%. Analyses no. 1, 2, and 4 pertain to grains of Os-dominant alloy, which corresponds to the mineral osmium. No. 3, 8, and 11: grains of Ir-dominant alloy, which corresponds to the mineral iridium. No. 5 and 6: grains of Ru-dominant alloy, which corresponds to the mineral ruthenium. No. 7, 9: rutheniridosmine. No. 10: PGE alloy phase, compositionally intermediate between the mineral ruthenium and rutheniridosmine. No. 12: lamella of Fe-bearing Ir-Ru-Os alloy hosted by an Os-Ir-Ru alloy phase poor in Fe. Zero indicates that amounts of elements are below detection limits.

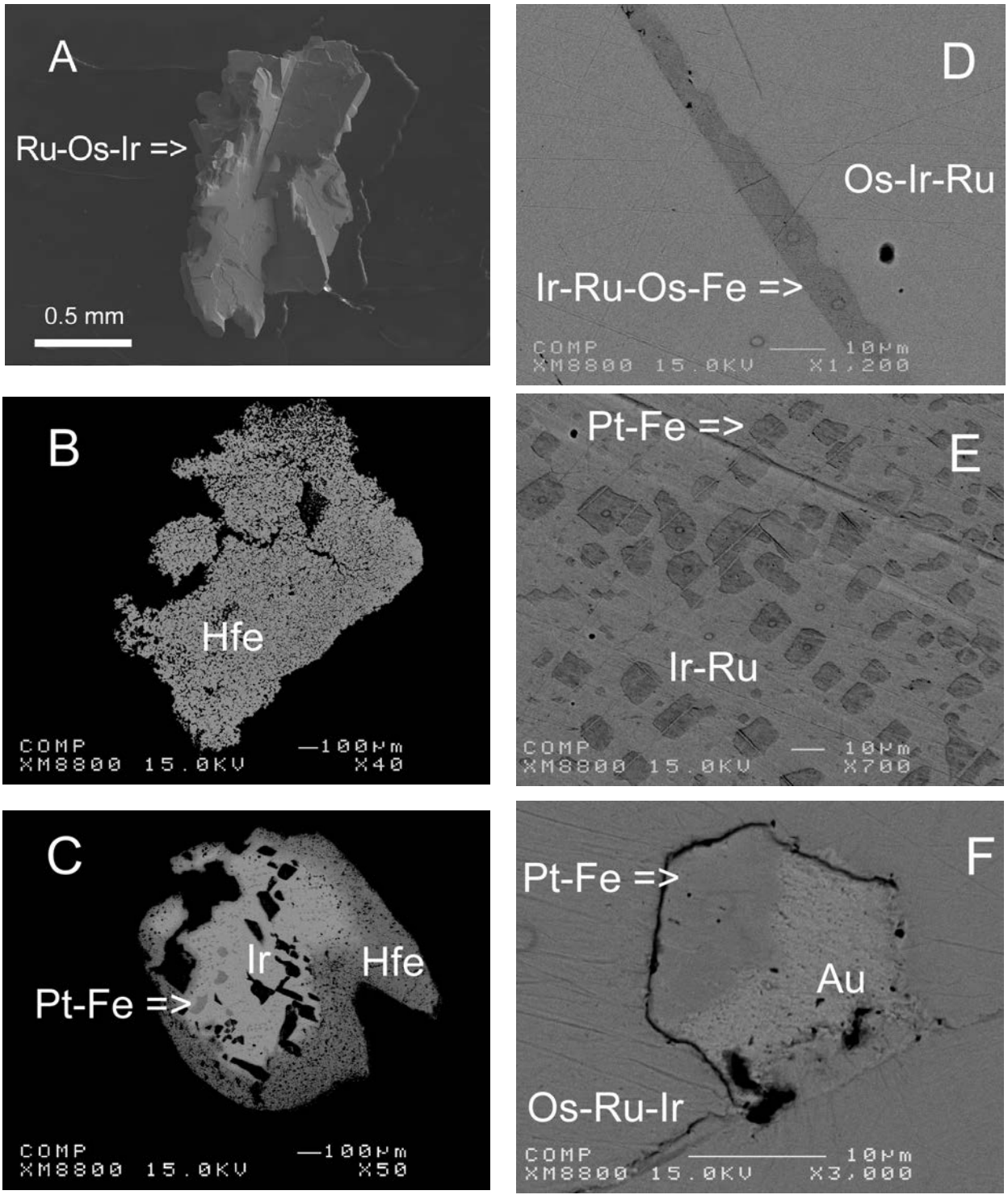

Figure 1. (**a**–**f**) Textural relationships of PGE-rich alloy minerals from the old collection, California. (**a**) A secondary electron image showing a faceted morphology of a grain of PGE alloy (Ru-Os-Ir), which consists of individual platelets of Ru-Os-Ir alloy. (**b**) A back-scattered electron image (BSE) showing a porous texture of a grain of hexaferrum, abbreviated as Hfe, a representative composition of which is $Fe_{0.38}Ir_{0.26}Ru_{0.20}Os_{0.15}$. (**c**) Hexaferrum enriched in Ir and having a composition $Fe_{0.38}Ir_{0.35}Os_{0.15}Ru_{0.08}$, is developed as a porous rim (Hfe) after an Ir-dominant Ir-Os-Ru alloy ($Ir_{0.56}Os_{0.20}Ru_{0.11}Pt_{0.06}Rh_{0.05}Fe_{0.01}$). Inclusions of Pt_3Fe-type alloy (Pt-Fe) are present in the Ir-dominant alloy (Ir). (**d**) An example of narrow lamella of Ir-Ru-Os alloy enriched in Fe (up to 4.6 wt%) that has exsolved from an Os-Ir-Ru alloy host poor in Fe. (**e**) Numerous inclusions of Pt_2Fe-type alloy (Pt-Fe) enclosed in a matrix of Ir-dominant alloy rich in Ru: ($Ir_{0.49}Ru_{0.29}Os_{0.09}Pt_{0.06}Fe_{0.03}Rh_{0.02}Ni_{0.01}$). (**f**) A subhedral inclusion of Pt_3Fe-type alloy (Pt-Fe), replaced by a Au-Ag alloy, which are hosted by an Os-Ru-Ir alloy. **b**–**f** = BSE images.

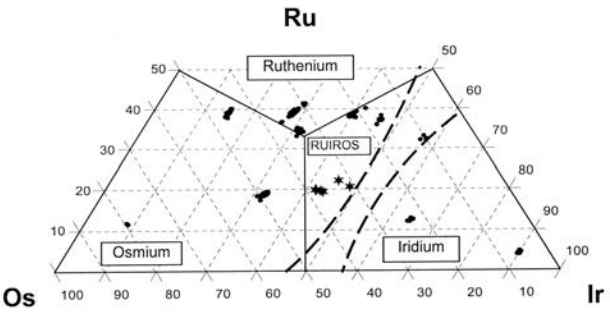

FIGURE 2. Variation in compositions of Os-Ru-Ir alloy minerals (W-free) and W-bearing rutheniridosmine from the old collection, California, in Os-Ru-Ir compositional space (atom proportions based on results of 351 EMP analyses: this study). The dashed lines show the miscibility gap of Harris and Cabri (1991) and Cabri et al. (1996); RUIROS is the compositional field of rutheniridosmine. (Circles = Os-Ru-Ir alloys (W-free); stars = W-rich rutheniridosmine.)

uniform values of their correlation coefficient *R*, calculated for Fe vs. Ru and Ru + Os ($R = –0.91$ and –0.92: Figs. 3a and 3d), indicative of a Fe-for-Ru substitution. One of these two grains, which is poorer in Fe, also exhibits a strongly negative Fe vs. Os correlation ($R = –0.90$), indicating a Fe-for-Os substitution, which does not exist, or is negligible, in the grains richer in Fe (Fig. 3b). All these observations suggest that Fe is incorporated via three mechanisms of element substitutions: Fe → Ru, Fe → (Os + Ru), and Fe → Ir. The latter mechanism operates only in the rim-like phase of the hexaferrum-rich solid solution, which is rich in Ir and displays a strongly negative Fe vs. Ir correlation ($R = –0.93$: Fig. 3c).

Additional results were obtained for a polycrystalline ring-like grain of the W-rich Os-Ir alloy having a ratio (Os + Ir)/(W + Mo) of 5:1, previously described by Barkov et al. (2006), which was repolished in this study to remove a relatively thick layer of the material. EMP data on newly analyzed micrograins of this ring-like grain gave a mean composition of $(Os_{4.03}Ir_{0.76}Fe_{0.21}Ru_{0.10})_{\Sigma 5.1}(W_{0.81}Mo_{0.07})_{\Sigma 0.9}$ (for $n = 29$: Σ atoms = 6). Contents of Pd, Pt, Rh, Ni, Co, and Cu are <0.01 apfu. These results (anal. 14 and 15, Table 2) are consistent with the previously reported compositions (Fig. 4). The presence of substantial Mo (up to 2 wt%), which correlates positively with W ($R = 0.75$), is confirmed. We document the existence of a new member in this compositional series, which has an Ir-dominant composition: $(Ir_{3.15}Os_{0.99}Fe_{0.23}Ru_{0.16})_{\Sigma 4.6}(W_{1.17}Mo_{0.27})_{\Sigma 1.4}$ (Figs. 4 and 5, anal. 16, Table 2). The size of individual micrograins of the W-rich phases,

TABLE 2. Compositions of Fe-Os-Ir-Ru, W-(Mo)-Os-Ir-Ru, and Pt-Fe alloys from the old collection, California

	Cu	Co	Fe	Ni	Pt	Ir	Os	Pd	Rh	Ru	W	Mo	Total
1	0	0	9.40	0.03	0.93	19.73	49.91	0	0.54	18.94	0	0	99.48
2	0	0.01	10.34	0	0.97	21.68	48.41	0.05	0.38	17.83	0	0	99.66
3	0.06	0	8.87	0	1.06	18.66	50.93	0.20	0.49	20.41	0	0	100.67
4	0.03	0.02	12.88	0	1.02	22.78	46.42	0	0.38	16.45	0	0	99.98
5	0	0.02	11.13	0.02	1.07	21.12	48.32	0.07	0.42	17.33	0	0	99.51
6	0	0	19.13	0	0.33	40.11	22.32	0.07	0.36	16.00	0	0	98.32
7	0	0.03	14.40	0	0.18	37.57	22.27	0	0.29	24.02	0	0	98.76
8	0	0.06	17.22	0.01	0.14	40.18	23.39	0	0.28	17.32	0	0	98.59
9	0.07	0.08	16.07	0.01	0.43	37.98	22.19	0.02	0.39	21.24	0	0	98.47
10	0.04	0	15.38	0.08	0.79	38.01	21.80	0	0.58	22.18	0	0	98.86
11	0.10	0	15.96	0.03	4.02	50.80	20.70	0	1.00	5.86	0	0	98.46
12	0.03	0	12.71	0.08	2.90	54.05	21.19	0	1.36	6.17	0	0	98.49
13	0.08	0.06	13.84	0.05	0.82	54.78	22.46	0.03	0.86	6.45	0	0	99.43
14	0	0	2.15	0.03	0	17.56	61.51	0.09	0	1.36	17.05	1.17	100.92
15	0.04	0	1.03	0.02	0.04	20.73	60.41	0.13	0	0.63	15.99	0.75	99.73
16	0.06	0	1.22	0	0.05	56.90	17.73	0.10	0.05	1.52	20.18	2.48	100.29
17	0.01	0	0.36	0.03	0	49.28	31.59	0	0.12	11.33	5.92	1.37	100.00
18	0.56	0.01	9.70	2.34	78.81	6.03	0.03	0	1.34	0.40	0	0	99.21
19	0.53	0	8.33	0.14	82.03	4.54	0.09	1.82	1.47	0.18	0	0	99.13
at%													
1	0	0	23.02	0.06	0.65	14.04	35.89	0	0.72	25.63	0	0	100
2	0	0.01	25.09	0	0.67	15.28	34.48	0.07	0.50	23.90	0	0	100
3	0.12	0	21.51	0	0.74	13.14	36.26	0.25	0.64	27.34	0	0	100
4	0.06	0.05	30.12	0	0.68	15.48	31.88	0	0.48	21.26	0	0	100
5	0	0.05	26.73	0.05	0.74	14.73	34.07	0.09	0.54	22.99	0	0	100
6	0	0	41.14	0	0.21	25.06	14.09	0.08	0.42	19.01	0	0	100
7	0	0.07	31.74	0	0.11	24.06	14.41	0	0.34	29.26	0	0	100
8	0	0.12	37.78	0.02	0.09	25.61	15.07	0	0.33	20.99	0	0	100
9	0.12	0.16	35.06	0.02	0.27	24.07	14.21	0.02	0.46	25.60	0	0	100
10	0.08	0	33.63	0.17	0.50	24.15	14.00	0	0.69	26.80	0	0	100
11	0.20	0	38.15	0.06	2.75	35.28	14.53	0	1.30	7.74	0	0	100
12	0.06	0	32.00	0.20	2.09	39.54	15.67	0	1.86	8.58	0	0	100
13	0.17	0.14	33.92	0.13	0.58	39.00	16.16	0.04	1.14	8.73	0	0	100
14	0	0	6.72	0.08	0	15.94	56.43	0.15	0	2.35	16.18	2.13	100
15	0.10	0	3.37	0.06	0.04	19.71	58.04	0.23	0	1.14	15.89	1.42	100
16	0.17	0	3.87	0	0.05	52.45	16.52	0.17	0.09	2.66	19.45	4.58	100
17	0.02	0	1.08	0.08	0	43.51	28.19	0	0.20	19.02	5.46	2.42	100
18	1.30	0.02	25.73	5.91	59.86	4.65	0.02	0	1.93	0.59	0	0	100
19	1.30	0	23.39	0.37	65.95	3.70	0.07	2.68	2.24	0.29	0	0	100

Notes: The selected results of WDS electron-microprobe analyses (JEOL JXA-8900 microprobe) are listed in wt% and in at%. Analyses no. 1–5, 6–10, and 11–13 pertain to three compositional series observed for three separate grains, consisting of Fe-Os-Ir-Ru solid solutions rich in the hexaferrum component. No. 14–16: unnamed $(Os,Ir)_5(W,Mo)$ and $(Ir,Os)_5(W,Mo)$. No. 17: W-(Mo)-bearing rutheniridosmine. No. 18 and 19: inclusions of Pt_2Fe- and Pt_3Fe-type alloys in Ir-Os-Ru alloys. Zero indicates that amounts of elements are below detection limits.

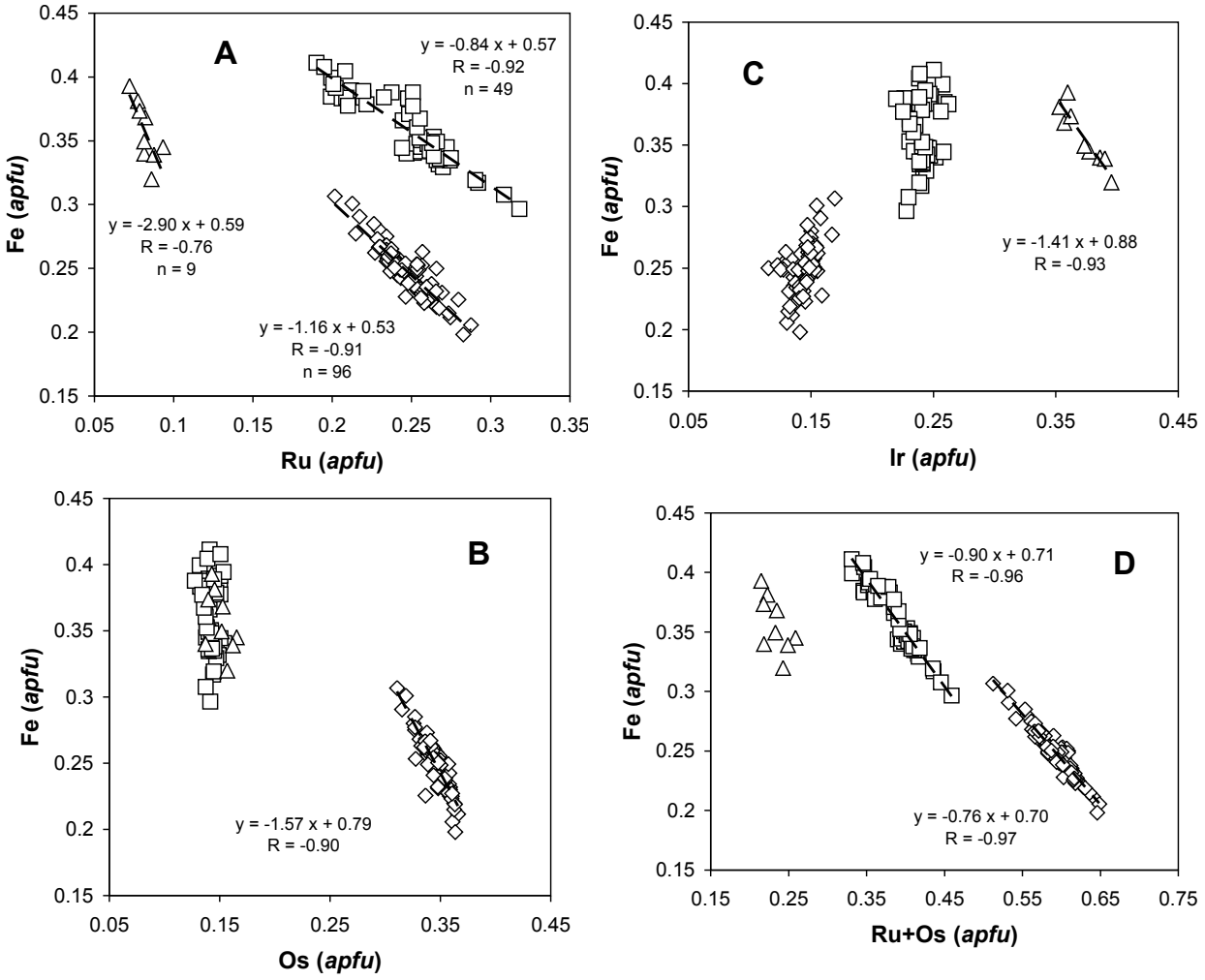

FIGURE 3. Correlations of (**a**) Fe vs. Ru, (**b**) Fe vs. Os, (**c**) Fe vs. Ir, and (**d**) Fe vs. Ru + Os in compositions of hexaferrum and Fe-rich Os-Ru-Ir alloys related to hexaferrum from the old collection, California. Results of EMP analyses (this study) are expressed in atoms per formula unit, apfu (basis: Σ atoms = 1).

which appear to be very hard, is commonly ≤5 μm. Six micrograins of W-bearing rutheniridosmine were also analyzed (Fig. 2, anal. 17, Table 2); they differ from the associated $(Os,Ir)_5(W,Mo)$ phases in a higher level of Ru (10.2–12.4 wt%), a lower level of W (5.9–7.6 wt%), and a low W/Mo, between 2.1 and 2.7.

Composition of the Pt-Fe and Au-Ag alloys, and of olivine inclusions

The Pt-Fe alloys occur in minor quantities, as small discrete grains of numerous inclusions (<50 μm in size: Fig. 1e) enclosed in a matrix phase of four grains of Ir- or Os-dominant alloys rich in Ru. Some of these inclusions display a slight preferred orientation, implying that these Pt-Fe alloys formed by exsolution from the matrix phase. Two compositional varieties of Pt-Fe alloys, of Pt_3Fe and Pt_2Fe type, were recognized (anal. 18, 19, Table 2); they are hosted by separate grains of Ir-Os-Ru alloy. These two populations of Pt-Fe alloy inclusions, in which the atomic ratio ΣPGE/(Fe + Cu + Ni) varies in the ranges 2.80–3.06 (n = 15) and 1.99–2.04 (n = 7), also differ in levels of minor elements: Pd (1.53–1.82 wt% vs. not detected) and Ni (0.14–0.30 vs. 2.27–2.39 wt%). The content of Ir is moderate and uniform in both of these varieties (up to about 6 wt%, or 5 at%). It is known that the solubility of Ir in Pt_3Fe decreases with decreasing temperature in the system Pt-Ir-Fe-S (Makovicky and Karup-Møller 2000).

The Pt_3Fe-type alloy (anal. 19, Table 2) corresponds to isoferroplatinum or Fe-rich platinum. No structural data could be obtained for the Pt-Fe alloys from California, because of their small grain-size. Isoferroplatinum, ideally Pt_3Fe, has an ordered primitive cubic (pc) structure, space group $Pm3m$. Similar atom proportions are known in Fe-rich platinum or "native Pt," having a disordered structure (fcc), space group $Fm3m$ (Cabri and Feather 1975). The Pt_2Fe alloy is unknown in experiments on the system Pt-Fe. However, natural examples of this alloy phase have been reported (Johan et al. 1989; Oberthür et al. 2002; Barkov et al. 2005; Melcher et al. 2005). The phase $Pt_{2.5}(Fe,Ni,Cu)_{1.5}$ was reported from the Tulameen complex, Canada (Nixon et al. 1990) and from Uralian-type complexes, Russia (Garuti et al. 2002). In addition, Malitch and Thalhammer (2002) described "homogeneous Pt_2Fe" with a disordered fcc structure. The existence of a clear miscibility-gap between the PtFe- and Pt_2Fe-type alloys

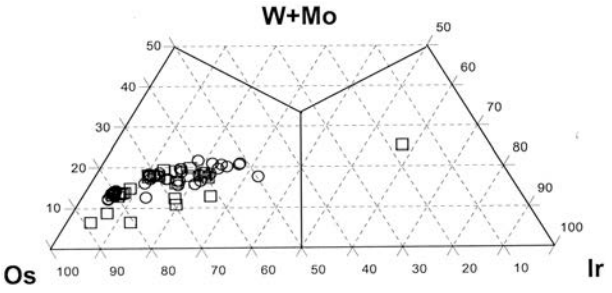

FIGURE 4. Compositional variation of the W-rich alloy of Os and Ir from the old collection, California, in Os-(W + Mo)-Ir compositional space. Atom proportions are based on results of 29 EMP analyses (squares = this study), compared with previously reported compositions (circles = Barkov et al. 2006).

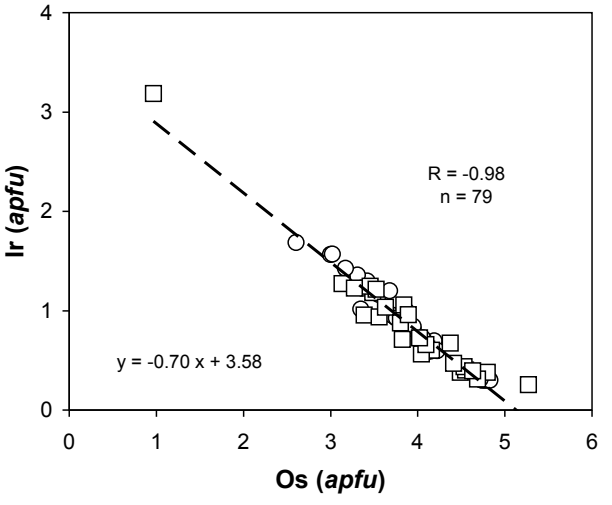

FIGURE 5. Correlation of Ir vs. Os in compositions of W-rich alloy of Os and Ir from the old collection, California (in apfu, based on Σ atoms = 6). The symbols are the same as those shown in Figure 4.

was documented for Pt-Fe alloy minerals from various placers of British Columbia; in contrast, no evidence was found for a miscibility gap between Pt_2Fe and Pt_3Fe (Barkov et al. 2008). The latter authors suggested that the Pt_2Fe-type phase is unlikely to be a distinct species of alloy, but rather is a compositional variant of Fe-rich platinum. Thus, the "stoichiometric" value of ΣPGE/(Fe + Cu + Ni) = 2 (anal. 18, Table 2) could reflect a lower limit of Pt content in the mineral platinum, or isoferroplatinum as a less probable alternative.

Micro-inclusions of Ag-Au alloy, typically subhedral (2–50 μm), enclosed within two grains of Ir- and Os-dominant alloys rich in Ru, vary in composition over the range $Au_{0.62–0.99}Ag_{0.01–0.37}Cu_{0–0.01}$ (n = 5), up to nearly pure gold: Cu <0.01, Ag 0.64, and Au 98.98 wt%. Their subhedral morphology suggests pseudomorphism after a pre-existing Pt-Fe alloy, as is evident from the observed replacement of Pt_3Fe by an Au-Ag alloy (Fig. 1f). The association between the PGE and Au-Ag is not unusual in some PGE deposits, especially those associated with the Noril'sk complex, Siberia (e.g., Barkov et al. 2000).

Two micro-inclusions of olivine (elongate, ca. 40 × 15 μm and droplet-like, ca. 30 μm) are hosted by the alloy phase $Os_{0.33}Ru_{0.33}Ir_{0.30}Pt_{0.03}Rh_{0.01}Fe_{<0.01}$, which is compositionally intermediate between Ir-rich osmium and ruthenium. Both of these inclusions are strongly magnesian. The mean composition and observed ranges (n = 5) are SiO_2 41.96 (41.75–42.28), Cr_2O_3 0.09 (0.06–0.12), FeO 4.29 (4.13–4.40), MnO 0.12 (0.10–0.13), MgO 53.15 (52.76–53.67), CaO 0.07 (0–0.12), NiO 0.27 (0.18–0.39), with a total 99.95 wt% (99.5–100.3 wt%), which correspond to $Fo_{95.2}$ ($Fo_{95.1–95.4}$).

DISCUSSION

The analyzed PGE alloy minerals from California, which are related compositionally to the systems Os-Ir-Ru, Fe-Os-Ir-Ru, W-(Mo)-Os-Ir-Ru, Pt-Fe, and Au-Ag, appear to have formed at several stages. The Os-Ir-Ru alloys, which correspond to the minerals osmium, iridium, ruthenium, and rutheniridosmine, probably crystallized as primary phases at magmatic temperatures. The exsolution-induced lamellae of Fe-bearing Ir-Ru-Os alloy (3.7–4.6 wt% Fe) and of Pt-Fe alloys (Pt_3Fe and Pt_2Fe) formed in the matrix of Os-Ir-Ru alloys poor in Fe as a result of a drop in temperature. We suggest that the Pt_2Fe alloy is a compositional variant of Fe-rich platinum, rather than a new (unnamed) species of alloy. The alteration-induced Fe-bearing Ir-Ru-Os alloy phase was probably produced in minor quantities along the grain margin, by a local reaction involving the primary Os-Ir-Ru alloy (Fe-poor) and a late-stage fluid or liquid enriched in Fe. Presumably, Au and Ag were incompatible components during crystallization of the host Ir-Os-Ru alloys. Relative levels of these elements must have attained a saturation level in microvolumes of residual Au-Ag-rich liquid at a final stage of crystallization. At this stage, minor amounts of pseudomorphous Au-Ag alloy, ranging up to $Au_{0.99}$, precipitated as a result of subsolidus reaction between the residual Au-Ag-rich liquid and the exsolution-induced Pt-Fe alloy phases (Fig. 1f).

The alloys analyzed in this study that are related to the systems Fe-Os-Ir-Ru and W-(Mo)-Os-Ir-Ru seem to be of secondary origin. These alloys are members of the hexaferrum series, W-(Mo)-bearing rutheniridosmine, and a series of unnamed compounds that extends from $(Os,Ir)_5(W,Mo)$ toward $(Ir,Os)_5(W,Mo)$. They were likely formed by the interaction of primary Os-Ir-Ru alloys with a reducing fluid phase, which remobilized Fe, W, and Mo during a metasomatic alteration, as is implied by the textural observations (Fig. 1c and Barkov et al. 2006). These exotic solid-solutions of the PGE have multicomponent compositions, which are anomalously enriched in unconventional elements, as a result of their metasomatic origin under conditions of low fugacities of O_2 and S_2, promoting the siderophile behavior of Fe, W, and Mo. The infiltration of fluids into the Trinity peridotite is reflected by the formation of metasomatic zones, involving serpentinization, which may imply metasomatic processes analogous to those known in subduction zones (Peacock 1987).

We have recognized three compositional series of solid solutions, which are rich in the hexaferrum component (Figs. 3a, 3c, and 3d). This occurrence of hexaferrum in California is the second occurrence worldwide of this species of hexagonal polymorph of native iron, reported only from the Alpine-type Chirynayskii dunite-harzburgite complex, Koryak Upland, Rus-

sia, the type locality (Mochalov et al. 1998). The composition of hexaferrum, which is a secondary phase (Fig. 1c), appears to depend on the composition of a primary Os-Ir-Ru alloy, at the expense of which it formed. A metallic iron component could be produced by destabilization and reduction of magnetite or titaniferous magnetite, reacting with CO in a reducing fluid phase: $Fe_3O_4 + 4CO \rightarrow 3Fe + 4CO_2$, or $Fe_{3-x}Ti_xO_4 + (4 - 2x)CO \rightarrow (3 - x)Fe + xTiO_2 + (4 - 2x)CO_2$ (e.g., Longbottom et al. 2006). Then, Fe^0 could be incorporated into the alloy phase $(Os, Ru, Ir)^0$ via the following mechanisms of element substitutions: Fe → Ru, Fe → (Os + Ru), or Fe → Ir, inferred from the observed compositional variations (Figs. 3a–3d).

The documented association of PGE alloys from California consists of species of Os-, Ir-, and Ru-rich alloy minerals. No grains of Pt-Fe alloys were found, which are the expected species in many PGE-bearing placer deposits. Here, the Pt-Fe alloys occur only as minor exsolution-induced phases. These features and, especially, the abundance of Ru-rich alloys (Tables 1 and 2), including rutheniridosmine and native ruthenium (Fig. 2), clearly point to an ophiolite origin of this association. In addition, no sulfide minerals were found, in spite of a careful examination. Thus, we infer that these Os-Ir-Ru alloy grains from California crystallized under conditions of a low fugacity of sulfur in ultramafic source-rocks poor in overall S. These rocks have a highly magnesian composition, as is implied by the composition of olivine inclusions, $Fo_{95.1–95.4}$, hosted by the Os-Ru-Ir alloy. The latter alloy host is very poor in Fe (mean content: 0.06 wt% for n = 31); thus, a re-equilibration between this host and olivine from the inclusions is unlikely the cause for the high values of Mg/(Mg + Fe) observed in this olivine. The extremely Fo-rich composition of these inclusions is a reflection of high-temperature reaction between chromite (or magnesiochromite) and a coexisting melt. As a result of this reaction, Fe was strongly partitioned into the chromite phase, causing a strong increase in Mg/(Mg + Fe) in the remaining melt, from trapped microdroplets of which the high-Mg inclusions subsequently crystallized. This suggestion is corroborated by observations from the Tulameen complex, British Columbia, in which the composition of olivine inclusions in PGE nuggets ($Fo_{93.2–95.2}$) closely corresponds to that of olivine grains from chromitites ($Fo_{92–95}$) and differs from that of olivine from host dunite-clinopyroxenite rocks: $Fo_{83–91}$ (Nixon et al. 1990). Note that the analyzed inclusions of olivine from California ($Fo_{95.1–95.4}$) closely correspond to the olivine (Fo_{95}) present in inclusions in PGE nuggets and chromitites of the Tulameen complex. We thus infer that the analyzed PGE-rich alloy grains from the old collection were likely derived from a mineralized zone of ultramafic-mafic rocks rich in chromite-magnesiochromite in the Trinity ophiolite complex of northern California.

ACKNOWLEDGMENTS

This study was made possible with financial support from the Natural Sciences and Engineering Research Council of Canada, which is gratefully acknowledged. We thank Daniel Ohnenstetter, an anonymous referee, and Edward Ghent, the associate editor, for their helpful and constructive comments and suggestions.

REFERENCES CITED

Barkov, A.Y., Martin, R.F., Poirier, G., Tarkian, M., Pakhomovskii, Y.A., and Men'shikov, Y.P. (2000) Tatyanaite, a new platinum-group mineral, the Pt analogue of taimyrite, from the Noril'sk complex (northern Siberia, Russia). European Journal of Mineralogy, 12, 391–396.

Barkov, A.Y., Fleet, M.E., Nixon, G.T., and Levson, V.M. (2005) Platinum-group minerals from five placer deposits in British Columbia, Canada. Canadian Mineralogist, 43, 1687–1710.

Barkov, A.Y., Fleet, M.E., Martin, R.F., Feinglos, M.N., and Cannon, B. (2006) Unique W-rich alloy of Os and Ir and associated Fe-rich alloy of Os, Ru, and Ir from California. American Mineralogist, 91, 191–195.

Barkov, A.Y., Martin, R.F., Fleet, M.E., Nixon, G.T., and Levson, V.M (2008) New data on associations of platinum-group minerals in placer deposits of British Columbia, Canada. Mineralogy and Petrology, 92, 9–29.

Bayliss, P., Kaesz, H.D., and Nickel, E.H. (2005) The use of chemical-element adjectival modifiers in mineral nomenclature. Canadian Mineralogist, 43, 1429–1433.

Cabri L.J. (2002) The Geology, Geochemistry, Mineralogy, and Mineral Beneficiation of Platinum-group Elements. Canadian Institute of Mining, Metallurgy and Petroleum, Special Volume 54, 852 p.

Cabri, L.J. and Feather, C.E. (1975) Platinum-iron alloys. Nomenclature based on a study of natural and synthetic alloys. Canadian Mineralogist, 13, 117–126.

Cabri, L.J., Harris, D.C., and Weiser, T.W. (1996) Mineralogy and distribution of platinum-group mineral (PGM) placer deposits of the world. Exploration and Mining Geology, 5, 73–167.

Garuti, G., Pushkarev, E.V., and Zaccarini, F. (2002) Composition and paragenesis of Pt alloys from chromitites of the Uralian-Alaskan-type Kytlym and Uktus complexes, northern and central Urals, Russia. Canadian Mineralogist, 40, 1127–1146.

Harris, D.C. and Cabri, L.J. (1991) Nomenclature of platinum-group-element alloys: Review and revision. Canadian Mineralogist, 29, 231–237.

Johan, Z., Ohnenstetter, M., Slansky, E., Barron, L.M., and Suppel, D. (1989) Platinum mineralization in the Alaskan-type intrusive complexes near Fifield, New South Wales, Australia. 1. Platinum-group minerals in clinopyroxenites of the Kelvin Grove prospect, Owendale intrusion. Mineralogy and Petrology, 40, 289–309.

Longbottom, R.J., Ostrovski, O., and Park, E. (2006) Formation of cementite from titanomagnetite ore. The Iron and Steel Institute of Japan (ISIJ), ISIJ International, 46, 641–646.

Makovicky, E. and Karup-Møller, S. (2000) Phase relations in the metal-rich portions of the phase system Pt-Ir-Fe-S at 1000 and 1100 °C. Mineralogical Magazine, 64, 1047–1056.

Malitch, K.N. and Thalhammer, O.A.R. (2002) Pt-Fe nuggets derived from clinopyroxenite-dunite massifs, Russia: a structural, compositional and osmium-isotope study. Canadian Mineralogist, 40, 395–418.

Melcher, F., Oberthür, T., and Lodziak, J. (2005) Modification and alteration of detrital platinum-group minerals from the eastern Bushveld complex, South Africa. Canadian Mineralogist, 43, 1711–1734.

Mochalov, A.G., Dmitrenko, G.G., Rudashevskii, N.S., Zhernovskii, V., and Boldyreva, M.M. (1998) Hexaferrum (Fe,Ru), (Fe,Os), (Fe,Ir)—A new mineral. Zapiski Vserossiiskogo Mineralogicheskogo Obshchestva, 127(5), 41–51 (in Russian).

Nixon, G.T., Cabri, L.J., and Laflamme, J.H.G. (1990) Platinum-group-element mineralization in lode and placer deposits associated with the Tulameen Alaskan-type complex, British Columbia. Canadian Mineralogist, 28, 503–535.

Oberthür, T., Weiser, T.W., Gast, L., Schoenberg, R., and Davis, D.W. (2002) Platinum-group minerals and other detrital components in the Karoo-age Somabula gravels, Gweru, Zimbabwe. Canadian Mineralogist, 40, 435–456.

Peacock, S.M. (1987) Serpentinization and infiltration metasomatism in the Trinity peridotite, Klamath province, northern California: implications for subduction zones. Contributions to Mineralogy and Petrology, 95, 55–70.

Snetsinger, K.G. (1971) Platinum-metal nugget from Trinity County, California. American Mineralogist, 56, 1101–1105.

MANUSCRIPT RECEIVED JANUARY 24, 2007
MANUSCRIPT ACCEPTED APRIL 25, 2008
MANUSCRIPT HANDLED BY EDWARD GHENT